Electronic Structure of Helicenes, C_2S Helicenes, and Thiaheterohelicenes

Yong-Hui Tian, Gyoosoon Park,† and Miklos Kertesz*

Department of Chemistry, Georgetown University, 37th & O Street, Washington, DC 20057-1227

Received September 29, 2007. Revised Manuscript Received February 8, 2008

The structures of linearly and ortho-fused helical polyaromatic hydrocarbon oligomers and polymers and their isoelectronic thiophene variants are studied using density functional theory (DFT). Structural and optical absorption data are compared with experiments where possible and excellent agreement is obtained. The results are interpreted with reference to orbital interaction diagrams. Infinite helicene tends to adopt a symmetry close to 6_1. C_2S helicene is predicted to have an approximately 26_3 symmetry leading to an interdigitated S···S network parallel to the helical axis. Thiaheterohelicene has an approximately 7_2 helical structure. Periodic boundary condition (PBC) calculation and highest occupied molecular orbital (HOMO)−lowest unoccupied molecular orbital (LUMO) gap extrapolation at the B3LYP/6-31G* level indicate a smaller band gap for helicene compared to phenacene. This difference is mainly due to the gap reducing effects of the transannular $\pi-\pi$ interactions across the helical pitch in helicene. The calculated band gap is much smaller for linear thienoacene than that for isomeric C_2S helicene due to the lack of effective conjugation pathway for the latter system. While thiaheterohelicene is structurally between the two large gap systems, helicene and C_2S helicene, its band gap is significantly lower than either of the two.

Introduction

Polycyclic aromatic hydrocarbons (PAHs) have received much interest as organic semiconducting materials.[1] One of the well studied series of these compounds is oligoacenes, which are linearly fused benzene rings as represented in **1** and **2**.

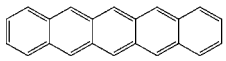

Pentacene (**1**)

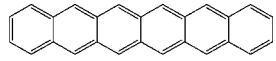

Hexacene (**2**)

The largest member of acenes synthesized so far is hexacene (**2**), the application of which is limited by its environmental instability. Higher member acenes, such as heptacene, are quite reactive.[2,3] Mondal et al. recently showed that heptacene with fair stability can be fabricated in a polymer matrix.[4] Among the oligoacenes, pentacene (**1**) is considered as the most promising molecular conductor and semiconductor due to its outstanding charge carrier mobility[5] with applications as organic field-effect transistors (OFETs). In order to understand the electronic properties, the electronic structure of oligoacene and hypothetical polyacene has attracted attention from many researchers. Tight binding calculation based on Hückel model predicted zero gap for polyacene.[6] However, Peierls distortion splits the degeneracy at the Fermi level[7] resulting in a small but nonzero band gap.

Another series of annulated oligoarenes is phenacenes, starting with phenanthrene (**3**), chrysene (**4**), and picene (**5**).

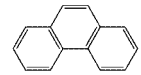

Phenanthrene (**3**)

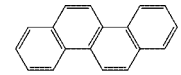

Chrysene (**4**)

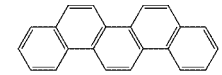

Picene (**5**)

Along with polyacenes, they can serve as models for the edge structure of graphene and carbon nanotubes.[8] Experimental[9] and theoretical[10] studies reveal that phenacenes are more stable than their isomeric acenes. Larger band gaps have been predicted for polyphenanthrenes than for polyacenes at various theoretical levels.[11] Topological effects were investigated to clarify the big band gap difference between the two systems.[12]

Helicenes represent the third series of PAHs isomeric to acenes and phenacenes. Helicenes, such as pentahelicene (**6**), hexahelicene (**7**) and [11]helicene (**8**) adopt a well-known

† Present address: Department of Chemistry, Kookmin University, 861-1, Chongnung, Songbuk, Seoul 136-702, Korea.

(1) Harvey, R. G. *Polycyclic Aromatic Hydrocarbons*; Wiley-VCH: New York, 1997.
(2) Boggiano, B.; Clar, E. *J. Chem. Soc.* **1957**, 2681.
(3) Bendikov, M.; Wudl, F.; Perepichka, D. F. *Chem. Rev.* **2004**, *104*, 4891.
(4) Mondal, R.; Shah, B. K.; Neckers, D. C. *J. Am. Chem. Soc.* **2006**, *128*, 9612.
(5) Dimitrakopoulos, C. D.; Malenfant, P. R. L. *Adv. Mater.* **2002**, *14*, 99.
(6) Longuett Higgins, H. C.; Salem, L. *Proc. R. Soc. London, Ser. A* **1960**, *255*, 435.
(7) (a) Raghu, C.; Anusooya Pati, Y.; Ramasesha, S. *Phys. Rev. B* **2002**, *65*, 155204. (b) Kertesz, M.; Hoffmann, R. *Solid State Commun.* **1983**, *47*, 97. (c) Houk, K. N.; Lee, P. S.; Nendel, M. *J. Org. Chem.* **2001**, *66*, 5517. (d) Srinivasan, B.; Ramasesha, S. *Phys. Rev. B* **1998**, *57*, 8927. (e) Cioslowski, J. J. *Chem. Phys.* **1993**, *98*, 473.
(8) Yoshizawa, K.; Yahara, K.; Tanaka, K.; Yamabe, T. *J. Phys. Chem. B* **1998**, *102*, 498.
(9) (a) Biermann, D.; Schmidt, W. *J. Am. Chem. Soc.* **1980**, *102*, 3163. (b) Biermann, D.; Schmidt, W. *J. Am. Chem. Soc.* **1980**, *102*, 3173.
(10) Wiberg, K. B. *J. Org. Chem.* **1997**, *62*, 5720.
(11) Kivelson, S.; Chapman, O. L. *Phys. Rev. B* **1983**, *28*, 7236.
(12) Liegener, C. M.; Bakhshi, A. K.; Ladik, J. *Chem. Phys. Lett.* **1992**, *199*, 62.

10.1021/cm702813s CCC: $40.75
Published on Web 04/24/2008

helical structure to accommodate the overcrowdedness of superposing rings.

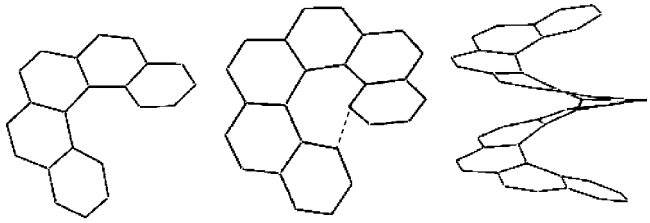

Pentahelicene **(6)** Hexahelicene **(7)** [11]helicene **(8)**

The helical pitch can be approximately defined as the distance of superposing carbon atoms across the overlapping rings as sketched in **7**. The first helicene model was proposed by Newman.[13] Since then, helicenes with larger number of rings up to 14 have been synthesized.[14] Helicenes have characteristic chiral properties arising from the helical structure.[15] However, little attention has been paid to their electronic structures, including the band gap (or HOMO−LUMO gap), of this system probably due to the nonplanarity of the helicene chain, which was suspected to be disadvantageous for π-electron conjugation. Semiempirical Hückel and INDO calculations suggested negligible transannular interaction between the overlapping rings across the helical pitch.[16] More recent DFT calculations indicated only a slight loss of aromatic character in helicenes despite of the nonplanarity as compared to the corresponding phenacenes.[17,18] In this paper, our discussion will focus on the comparison of electronic structure between the helical vs linear series as a function of size.

α-Oligothiophenes constitute another class of widely used π-conjugated systems.[19] Their applications run a broad spectrum including light-emitting diodes,[20] film transistors,[21] and electroactive materials.[22] Exploration of the potential surface[23] of polythiophenes indicated two local minima corresponding to the planar anti conformation and the helical *syn* conformation as shown by **9** and **10**.

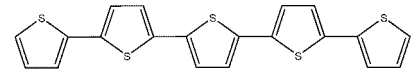

α-thiophene with *anti* conformation **(9)**

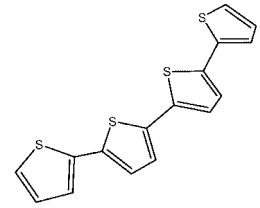

α-thiophene with helical *syn* conformation **(10)**

The isomeric β-oligothiophenes attracted less attention possibly because of the lower degree of delocalization[24] due to the steric repulsion between neighboring rings. Correspondingly, two series of fused oligothiophenes exist. The straight quasi-linear oligothienoacenes, such as heptathienoacene (**11**), arise from the annulation of α-oligothiophenes. The hypothetical polymer is represented with the formula of $(C_2S)_n$.[25]

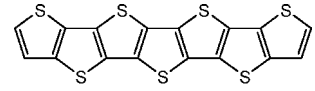

Heptathienoacene **(11)**

A series of oligothienoacenes up to 8 thiophenes rings have been synthesized.[26] Thienoacenes tend to be more planar and thereby more conjugated than α-oligothiophene. In the crystal structure, oligothienoacenes favor more pronounced $\pi-\pi$ stacking[26a] due to the lower ratio of C−H bonds. Such features are suggested to be favorable for charge carrier mobility, which is important for electronic and optoelectronic applications.[27]

Another $(C_2S)_n$ isomer is C_2S helicene (**12**) derived from the annulation of β-oligothiophenes.

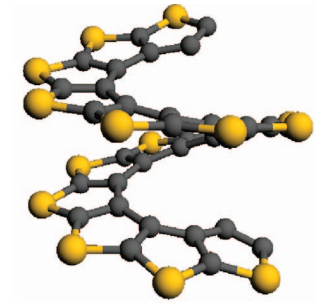

C_2S helicene **(12)**, terminal groups are not shown

A series of helical $(C_2S)_n$oligomers have been recently synthesized by Rajca and Miyasaka et al.[28] The electronic

(13) (a) Newman, M. S.; Lednicer, D. *J. Am. Chem. Soc.* **1956**, *78*, 4765. (b) Newman, M. S.; Darlak, R. S.; Tsai, L. L. *J. Am. Chem. Soc.* **1967**, *89*, 6191.
(14) (a) Martin, R. H. *Angew. Chem., Int. Ed.* **1974**, *13*, 649. (b) Martin, R. H.; Bayes, M. *Tetrahedron* **1975**, *31*, 2135.
(15) Peyerimhoff, S. D. *Interactions in molecules: electronic and steric effects*; Wiley-VCH: New York, 2003.
(16) (a) Obenland, S.; Schmidt, W. *J. Am. Chem. Soc.* **1975**, *97*, 6633. (b) Deb, B. M.; Kavu, G. *Can. J. Chem.* **1980**, *58*, 258.
(17) Schulman, J. M.; Disch, R. L. *J. Phys. Chem. A* **1999**, *103*, 6669.
(18) Portella, G.; Poater, J.; Bofill, J. M.; Alemany, P.; Sola, M. *J. Org. Chem.* **2005**, *70*, 2509.
(19) Fichou, D. *Handbook of Oligo- and Polythiophene*; Wily-VCH: New York, 1999.
(20) Gross, M.; Müller, D. C.; Nothofer, H.-G.; Scherf, U.; Neher, D.; Bräuchle, C.; Meerholz, K. *Nature* **2000**, *405*, 661.
(21) Pappenfus, T. M.; Chesterfield, R. J.; Frisbie, C. D.; Mann, K. R.; Casado, J.; Raff, J. D.; Miller, L. L. *J. Am. Chem. Soc.* **2002**, *124*, 4184.
(22) Yu, H.-h.; Xu, B.; Swager, T. M. *J. Am. Chem. Soc.* **2003**, *125*, 1142.
(23) Cui, C. X.; Kertesz, M. *Phys. Rev. B* **1989**, *40*, 9661.
(24) (a) Ye, X.-S.; Wong, H. N. C. *J. Org. Chem.* **1997**, *62*, 1940. (b) Kauffmann, T.; Greving, B.; König, J.; Mitschker, A.; Woltermann, A. *Angew. Chem., Int. Ed. Engl.* **1975**, *14*, 713. (c) Kauffmann, T. *Angew. Chem., Int. Ed. Engl.* **1979**, *18*, 1.
(25) Oyaizu, K.; Iwasaki, T.; Tsukahara, Y.; Tsuchida, E. *Macromolecules* **2004**, *37*, 1257.
(26) (a) Zhang, X.; Côté, A. P.; Matzger, A. J. *J. Am. Chem. Soc.* **2005**, *127*, 10502. (b) Okamoto, T.; Kudoh, K.; Wakamiya, A.; Yamaguchi, S. *Chem. Eur. J.* **2007**, *13*, 548.
(27) (a) Mazzeo, M.; Vitale, V.; Della Sala, F.; Anni, M.; Barbarella, G.; Favaretto, L.; Sotgiu, G.; Cingolani, R.; Gigli, G. *Adv. Mater.* **2005**, *17*, 34. (b) Xiao, K.; Liu, Y.; Qi, T.; Zhang, W.; Wang, F.; Gao, J.; Qiu, W.; Ma, Y.; Cui, G.; Chen, S.; Zhan, X.; Yu, G.; Qin, J.; Hu, W.; Zhu, D. *J. Am. Chem. Soc.* **2005**, *127*, 13281.
(28) (a) Rajca, A.; Miyasaka, M.; Pink, M.; Wang, H.; Rajca, S. *J. Am. Chem. Soc.* **2004**, *126*, 15211. (b) Miyasaka, M.; Rajca, A.; Pink, M.; Rajca, S. *J. Am. Chem. Soc.* **2005**, *127*, 13806. (c) Miyasaka, M.; Rajca, A. *J. Org. Chem.* **2006**, *71*, 3264.

structure of linear oligothienoancene (**11**) has been explored at the semiempirical PM5 level,[25] and to the best of our knowledge, such investigations on helically annealed β-thiophenes have not been reported. Herein, we explore the factors affecting the band gap (or the HOMO−LUMO gaps) for the two series of fused thiophene oligomers and related hypothetical polymers based on DFT calculations and qualitative orbital analysis.

Another related group of helical molecules are conjugated thiaheterohelicenes, in which thiophene and benzene rings are ortho-fused in an alternating fashion as displayed by hexathiahetero[11]helicene (**13**).[29] A significant advantage of such helical conjugated molecules is their established synthesis and good yield.[30,31] The presence of sulfur atoms in the helicene backbone offers opportunities to modify their electronic, linear and nonlinear optical properties.[32]

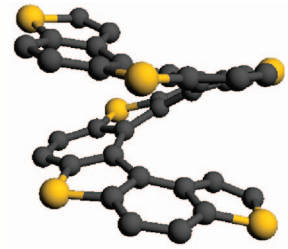

Hexathiahetero[11]helicene **(13)**, terminal Hs are not shown.

In this article, structural and electronic properties were investigated at DFT level covering helicenes, C_2S helicenes and thiaheterohelicenes. Further calculations were also performed on phenacenes and thienoacenes due to their structural similarity to isomeric helicenes and C_2S helicenes, respectively. The band gaps were calculated from oligomer extrapolations and with periodic boundary condition (PBC) calculation if possible. The calculated results were compared with structural and optical experiments wherever data are available helping to control the reliability of the theory level we used.

Computational Methodology

All DFT calculations were performed with the Gaussian 03 program.[33] The geometry optimizations were carried out with Becke's three parameter (B3) hybrid exchange functionals combined with Lee−Yang−Parr (LYP) correlation functionals (B3LYP).[34] For a series of shorter oligophenacenes and oligothienoacenes, the unconstrained geometry optimization gave rise to C_{2v} and C_{2h} symmetry for oligomers with odd and even number of rings respectively, in agreement with the corresponding X-ray structures. Therefore, geometry optimization was constrained with C_{2v} or C_{2h} symmetry for larger oligomers. The geometry optimization on helicenes, C_2S helicenes and thiaheterohelicenes was constrained to a C_2 geometry based on similar validation for phenacenes and thienoacenes. The geometry was also optimized with PBC calculations for the phenacene and thienoacene polymer at the same level as for the corresponding oligomers.

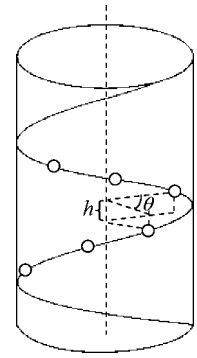

Figure 1. Illustration of the screw axis of operation for a helical system.

For helical systems, the screw operation is characterized by a rotation θ and a translation h per repeat unit along the screw axis as shown in Figure 1.[35] A helical system remains invariant if one repeats the screw operation l times (l is an integer), which corresponds to a rotation of $2\pi ql$ followed by a translation of $a = lh$, where $\theta 2 = \pi q$ is defined as the rotation angle. If q is a rational number (m/n), then translational symmetry can be defined along the screw axis (usually denoted as m_n), and periodic boundary conditions can also be defined. When q is an irrational number, translational symmetry does not exist. For infinite phenacene and thienoacene, $\theta = \pi$, $q = 1/2$, and the translational vector along the screw axis has the length of $a = 2h$. For helicenes, PBC calculations were performed based upon the fact that, as discussed in the next section, helicene has a close to 6_1 symmetry, which means $l = 6$, $q = 1/6$, and $a = 6h$. The symmetries of C_2S helicenes and thiaheterohelicenes are close to 26_3 and 7_2, respectively. PBC calculations would be possible but costly in these cases, because of the large number of atoms in each translational unit cell.

Band gaps were calculated through two supplementary approaches, HOMO−LUMO gap extrapolations for oligomers and PBC calculations for polymers. All geometries were fully optimized except for the imposed translational symmetry in the PBC calculations. We used the B3LYP hybrid density functional with the 6-31G* basis set. The applicability of B3LYP/6-31G* to geometry optimization and to band gap calculations has been discussed,[36,42] and it was suggested to predict values in good agreement with experiment for various π-conjugated systems.[37]

Semiempirical periodic calculations were carried out for all systems studied in this paper using the Longuet−Higgins

(29) (a) Yamada, K.; Tanaka, H.; Nakagawa, H.; Kawazura, H. *Chem. Lett.* **1981**, 343. (b) Caronna, T.; Catellani, M.; Luzzati, S.; Malpezzi, L.; Meille, S. V.; Mele, A.; Richter, C.; Sinisi, R. *Chem. Mater.* **2001**, *13*, 3906.
(30) Wynberg, H.; Groen, M. B.; Schadenberg, H. *J. Org. Chem.* **1971**, *36*, 2797.
(31) Bossi, A.; Maiorana, S.; Baldoli, C.; Graiff, C.; Tiripicchio, A.; Licandro, E. *Eur. J. Org. Chem.* **2007**, *27*, 4499.
(32) Champagne, B.; Andre, J. M.; Botek, E.; Licandro, E.; Maiorana, S.; Bossi, A.; Clays, K.; Persoons, A. *ChemPhysChem* **2004**, *5*, 1438.
(33) Frisch, M. J.; et al. *Gaussian 03*, revision D.01; Gaussian, Inc.: Pittsburgh, PA, 2003.
(34) (a) Becke, A. D. *J. Chem. Phys.* **1993**, *98*, 5648. (b) Lee, C.; Yang, W.; Parr, R. G. *Phys. Rev. B* **1988**, *37*, 785.
(35) Cui, C. X.; Kertesz, M. *J. Am. Chem. Soc.* **1989**, *111*, 4216.
(36) Salzner, U.; Lagowski, J. B.; Pickup, P. G.; Poirier, R. A. *J. Comput. Chem.* **1997**, *18*, 1943.
(37) Yang, S.; Kertesz, M. *J. Phys. Chem. A* **2006**, *110*, 9771.
(38) Longuet-Higgins, H. C.; Salem, L. *Proc. R. Soc. London, Ser. A* **1959**, *251*, 172.

and Salem (LHS) method[38] in order to develop a qualitative orbital analysis.[39] The LHS method is a semiempirical model with one π orbital per each C and S atom, in which only π-electrons are considered within the tight-binding (Hückel) approximation using bond distance dependent transfer (resonance) integrals. The calculations in this article are based on the LHS model parametrized by Kürti and Surjan.[40] All geometries were relaxed in the LHS calculations. The translational unit cells of phenacene and thienoacene contain two unit cells defined by the screw axis of symmetry. This leads to a 2-fold back-folded band structure for the PBC calculation at the DFT level compared to that at the LHS level, in which the unit cells are related by the screw axis of symmetry. For helicenes, assuming a 6_1 symmetry, the unit cell is six-times larger at the DFT level compared to that at the LHS level because the translational unit cell contains six C_4H_2 units based on the screw axis of symmetry. Correspondingly, the reciprocal lattice vector for PBC calculation at DFT level is six times smaller than that at the LHS level, but due to the backfolding, it has six times as many energy bands. The notation in the band structures reflects this difference: in the LHS bands, the k space varies from 0 to π/h, while in the translational PBC based DFT calculations it varies from 0 to π/a ($a = 6h$). The DFT bands are presented in the reduced Brillouin zone (BZ) where the translational unit cell has the length of $a = 2h$ or $6h$. For comparison, we will present the band structure of the LHS model both in the reduced BZ and in some cases also in the extended (0 to π/h) BZ. In the band structure diagrams, only bands originating from the π electrons are given. On some band diagrams, band crossings occur due to band backfolding. For one-dimensional periodic systems with a translational vector of h, when the unit cell is enlarged n-fold, the corresponding translational vector is also increased to $a = nh$. Then, the BZ is reduced to the range of $[-\pi/a, \pi/a]$ to $[-\pi/nh, \pi/nh]$, which is called reduced BZ. The original zone of $[\pi/h, \pi/h]$ is called the extended zone. Each band in the reduced BZ can be obtained by "backfolding" n-times the bands in the extended BZ.[41] Some of these backfolded bands may cross each other in the reduced BZ, if they happen to have the same energy in the extended BZ. However, for the bands, which avoid a crossing in the extended BZ, the avoided crossing is also reflected in the folded bands in the reduced BZ.

Results and Discussion

In the next sections, the discussion was divided into three parts, phenacene and helicene; thienoacene and C_2S helicene; and thiaheterohelicene aiding the comparison between the corresponding linear and helical molecules. In each section we discuss the geometry, the electronic structure and their relationships.

Geometry Optimization of Phenacenes and Helicenes. The HOMO−LUMO gap or band gap is dependent on the geometry, especially on bond length alternation (BLA). It is commonly accepted that Hartree−Fock (HF) and local spin density approximation (LSDA) overestimates and underestimates BLA, respectively, while DFT with hybrid functionals such as B3LYP predicts more realistic intermediate BLA values.[42] Table 1 lists the characteristic bond distances of chrysene (**4**) and [11]helicene (**8**).

Table 1. Bond Distances for Chrysene (4) and [11]Helicene (8) from Crystal Structure and Geometry Optimization Using B3LYP/6-31G*[a]

		unit (Å)					
		a	b	c	d	e	f
chrysene (**4**)	optimization	1.364	1.427	1.428	1.453	1.418	1.431
	X-ray[43]	1.331	1.417	1.417	1.453	1.402	1.437
[11]helicene (**8**)	optimization	1.369	1.429	1.427	1.452	1.427	1.429
	X-ray[44]	1.348	1.420	1.427	1.451	1.413	1.425

[a] The bond distances in the middle rings are labeled in Figure 2. For [11] helicene, the geometry was optimized with a C_2 symmetry constraint.

Table 2. Helical Pitches from Experimental Geometries and Optimizations at B3LYP/6-31G*[a]

	helical pitch (Å)		
	inner	outer	average
[11]helicene, X-ray[b]	3.442	3.980	3.711
[11]helicene, optimization	3.540	3.839	3.690
[30]helicene, optimization	3.677	3.717	3.697
PBC optimization (6_1 symmetry)	$a = 6h = 3.691$		

[a] The inner and outer values correspond to the distances between the superposed carbon atom pairs on the inside and the periphery of the helix, respectively. [b] Reference 44.

These two molecules are the largest ones for the phenacene and helicene series, available in the Cambridge Structural Database (CSD). (The X-ray structure for picene (**5**) appears erroneous,[45] since the a-type peripheral bond is not the shortest in the middle ring in ref 45.). Only the bond distances in the middle rings are listed, because they are least affected by end effects. For helicenes, the shortest carbon−carbon (CC) contacts across the helical pitch are around the van der Waals distance of carbon. For example, the shortest CC distance is 3.14 Å, a mean value from 36 hits with a hexahelicene scaffold in CSD.[46] The shortest CC distance in [11] helicene is around 3.4−3.5 Å as shown in Table 2. It is well-known that DFT at the level used here is usually unable to describe dispersion forces accurately. However, it still predicts accurately the bond distances as listed in Table 1. The optimized geometries fit well with the experimental values. Coincidently, the optimized helical pitch values for [11]helicene are in fair agreement with the X-ray structural data as presented in Table 2.

We conclude that B3LYP/6-31G* is sufficiently reliable for geometry optimization for these systems. To examine the constraint of PBC on the optimized geometry, relatively longer oligomers were optimized, and the bond distances on

(39) Whangbo, M.-H.; Hoffmann, R.; Woodward, R. B. *Proc. R. Soc. London, Ser. A* **1979**, *366*, 23.
(40) Kurti, J.; Surjan, P. R. *Springer Ser. Solid-State Sci.* **1989**, *91*, 69.
(41) Hoffmann, R. *Solids And Surfaces: A Chemist's View Of Bonding In Extended Structures*; VCH: New York, 1997; p 83.
(42) Kertesz, M.; Choi, C. H.; Yang, S. *Chem. Rev.* **2005**, *105*, 3448.
(43) Krygowski, T. M.; Ciesielski, A.; Swirska, B.; Leszczynski, P. *Pol. J. Chem.* **1994**, *68*, 2097.
(44) Le Bas, G.; Navaza, A.; Knossow, M.; Rango, C. *Cryst. Struct. Commun.* **1976**, *5*, 713.
(45) De, A.; Ghosh, R.; Roychowdhury, S.; Roychowdhury, P. *Acta Crystallogr., Sect. C* **1985**, *41*, 907.
(46) Wachsmann, C.; Weber, E.; Czugler, M.; Seichter, W. *Eur. J. Org. Chem.* **2003**, 2863.

Table 3. Optimized Bond Distances (in Å) for Infinite Phenacene and Helicene Using PBC and for the Central Rings of [25]Phenacene and [30]Helicene at B3LYP/6-31G*[a]

	a	b	c	d
phenacene (PBC−DFT)	1.367	1.425	1.419	1.449
[25]phenacene	1.367	1.425	1.420	1.449
helicene (PBC−DFT)[b]	1.363	1.426	1.426	1.456
[30]helicene	1.365	1.427	1.424	1.454

[a] The bond distances are labeled as in Figure 2. [b] Assuming a 6_1 helix.

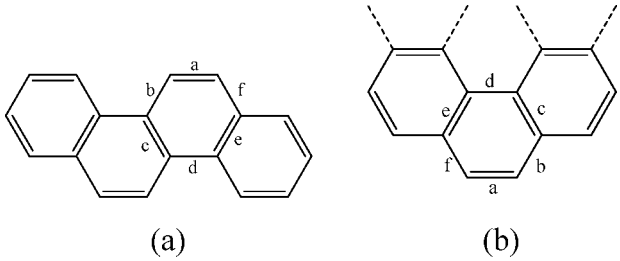

Figure 2. Bond distance labels used in Table 1: (a) chrysene (**4**); (b) [11]helicene (**8**).

the middle ring were compared with the corresponding distances optimized using PBC. [25]phenacene and [30]helicene were chosen for this purpose. The two approaches gave nearly the same bond distances for both phenacene and helicene as presented in Table 3. While these systems display aspects of delocalized π-electron conjugation, oligomers of the size of 25 and 30 rings are sufficiently long to display the key characteristics of the infinite systems. This finding is useful, especially in the cases where periodic calculations are not practical, as discussed for the sulfur containing helicenes later on.

For helicenes, our calculations for a series of oligomers indicated that the helicene chain approached an approximate 6_1 symmetry as the number of rings increased. Therefore, the unit cell can be limited to a reasonable size ($6 \times C_4H_2 = C_{24}H_{12}$) making the PBC−DFT computation practical. The optimized helical pitch values are listed in Table 2. The rings tilt inward for shorter oligomers like [11]helicene, and tend to become more parallel for longer oligomers as shown for [30]helicene. Despite the tilt, the average pitch values for both [11]- and [30]helicene are similar to the pitch from the PBC calculation, and are close to the experimental values for [11]helicene. Some double bond localization can be observed in both systems at the peripheral a-type bonds (as labeled in Figure 2). The longest bonds occur at the "inner" d-type bonds. The corresponding bond distances are very close for infinite phenacene and infinite helicene as shown in Table 3.

Band Gap of Phenacenes and Helicenes. Two complementary approaches were employed to calculate the band gap, E_g. The first is based on the HOMO−LUMO energy difference of oligomers, and the second comes from PBC calculations of the infinite polymer model. The HOMO−LUMO gaps were calculated with B3LYP/6-31G* for a series of oligomers containing up to 26 and 30 rings for phenacenes and helicenes, respectively. The band gaps for the polymers were obtained by extrapolating to infinite size from the

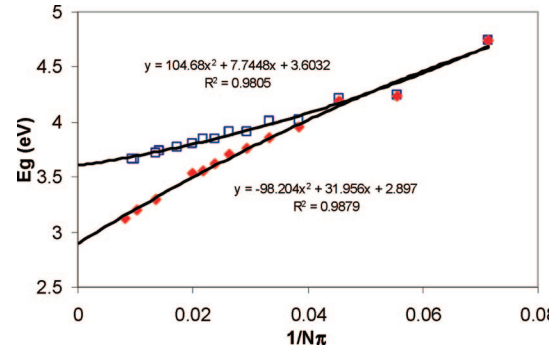

Figure 3. B3LYP/6-31G* calculated HOMO−LUMO gaps for oligomers of phenacenes (squares) and helicenes (diamonds) as a function of $1/N\pi$. $N\pi$ is the number of π electrons. Quadratic fits and the corresponding statistics are also shown. Oligomers with up to 26 and 30 rings were used for phenacenes and helicenes, respectively.

Table 4. Calculated Band Gaps for Phenacene and Helicene (in eV)[a]

	HOMO−LUMO extrapolation, DFT [b]	PBC−DFT	PBC−LHS
phenacene	3.60	3.59	2.55
helicene	2.90	2.90	2.70

[a] HOMO−LUMO gaps and PBC−DFT gaps were calculated at the B3LYP/6-31G* level and compared with the PBC calculations at the LHS level. [b] Extrapolation range: phenacene, 3−26 rings; helicene, 3−30 rings.

oligomer data.[47–49] Figure 3 shows the quadratically fitted HOMO−LUMO gap values as a function of the reciprocal of the number of π electrons for phenacene and helicene systems.

Table 4 lists the band gaps obtained by the two approaches. The extrapolated band gap for helicenes is 2.90 eV, while that for phenacenes is 3.60 eV. PBC calculation indicated a direct band gap of 3.59 eV for phenacene, and an indirect band gap of 2.90 eV for helicene. These two pairs of values obtained by the two different routes for each system are sufficiently close to accept them as essentially converged values. The optical band gap obtained from experiments is 2.5 eV for helicene (extrapolated by λ_{max} vs $1/n$, $n = 6-9$),[50] which is smaller than the calculated value, 2.9 eV. One of the possible reasons is that for the HOMO−LUMO method, the optical absorption is approximated by the one electron vertical excitation from the HOMO of the ground-state to the virtual orbital represented by LUMO. Therefore, HOMO−LUMO gap is larger than the experimental optical absorption, which includes the exciton transition energy. The argument is supported by the fact that the calculated absorption spectra by TD-DFT method are in good agreement with experiment for [n]helicene ($n = 4-7$ and 12).[51,52] As far as the band gap is concerned, the assumption of the perfect 6_1 helix structure for the infinite helicene also appears as a reasonable approximation. Due to the overcrowdedness of helicene molecules across the helical pitch, the helicene chain is nonplanar; therefore the conjugation is partially

(47) Yang, S.; Olisheviski, P.; Kertesz, M. *Synth. Met.* **2004**, *141*, 171.
(48) Zade, S. S.; Bendikov, M. *Org. Lett.* **2006**, *8*, 5234.
(49) Gierschner, J.; Cornil, J.; Egelhaaf, H.-J. *Adv. Mater.* **2007**, *19*, 173.
(50) Rajca, A.; Rajca, S.; Pink, M.; Miyasaka, M. *Synlett.* **2007**, 1799.
(51) Furche, F.; Ahlrichs, R.; Wachsmann, C.; Weber, E.; Sobanski, A.; Vögtle, F.; Grimme, S. *J. Am. Chem. Soc.* **2000**, *122*, 1717.
(52) Rulisek, L.; Exner, O.; Cwiklik, L.; Jungwirth, P.; Stary, I.; Pospisil, L.; Havlas, Z. *J. Phys. Chem. C* **2007**, *111*, 14948.

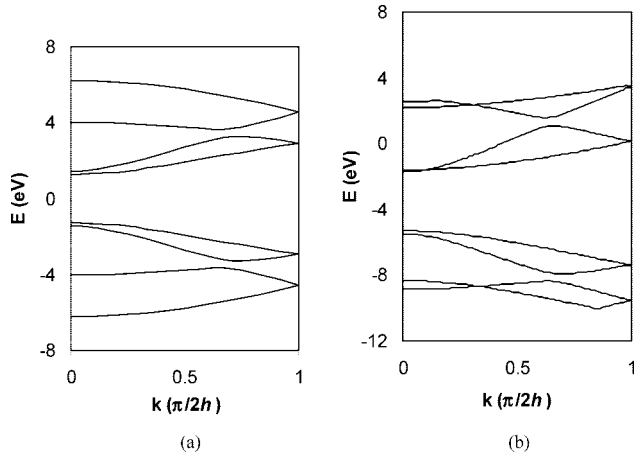

Figure 4. Calculated band structure of phenacene. (a) Back-folded bands at the LHS level; (b) PBC bands at B3LYP/6-31G* level. Four occupied and four empty π-bands are shown.

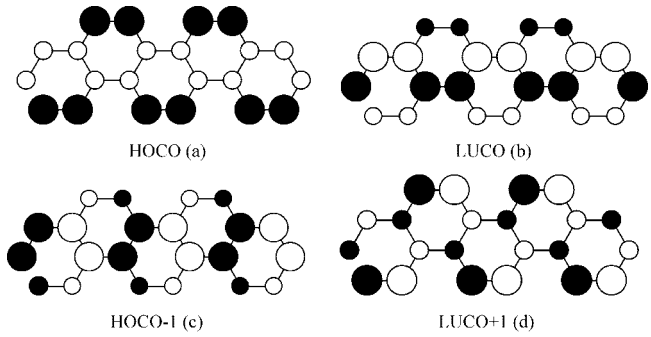

Figure 5. Illustration of orbital diagrams at $k = 0$ for infinite phenacene, corresponding to Figure 4b.

reduced. Therefore, the HOMO−LUMO gaps of helicenes might be expected to be larger than those of the corresponding phenacenes. However, for the systems larger than six rings, helicenes have smaller HOMO−LUMO gaps than phenacenes as shown in Figure 3.

The 2-fold back-folded band structure calculated with the LHS model is shown in Figure 4a. The DFT calculated band structure for phenacene is shown in Figure 4b. Note that the band crossing for phenacene is symmetry forbidden in Figure 4. The avoided crossing can be clearly seen from the band plot in the extended BZ (see Figure 3 in the Supporting Information). The similarity between the two band structures suggests that the semiempirical LHS model is capable to predict qualitatively the electronic properties of this extended system. Both of them indicate a direct band gap at $k = 0$, and qualitatively, the overall bandwidth values are similar.

In order to analyze the geometrical and electronic structures, a qualitative orbital analysis has been performed. The highest occupied crystal orbitals (HOCO) and lowest unoccupied crystal orbitals (LUCO) at $k = 0$ were constructed from atomic π orbitals, which are shown in Figure 5a,b. The nodal pattern of the HOCO indicates a dominant contribution from the isolated ethylene HOMO orbital located on the a-type bonds as labeled in Figure 2, while the nodal pattern of LUCO is characteristic of a quinonoid form of *cis*-PA composed of the c-type and d-type bonds.[25] According to the *fully optimized* geometry, the peripheral a-type bonds are highly localized resulting in a lower HOCO level. The

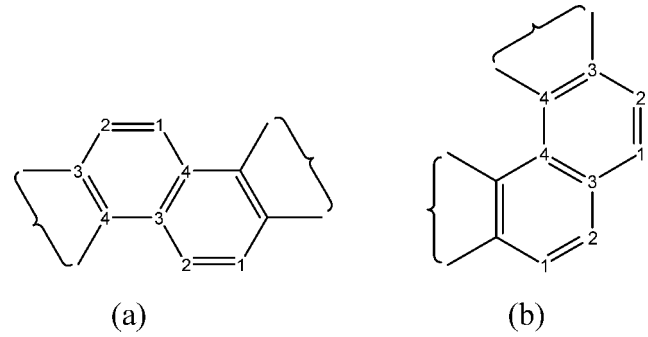

Figure 6. Illustration of bond connectivities in phenacenes (a) and helicenes (b) for LHS calculations. Numbering is given for two adjacent unit cells.

optimized central d-type bonds are stretched significantly (compared to standard C=C bonds, or a-type bonds) and the degree of bonding character is reduced on these bonds, which leads to higher LUCO level. Therefore, unsubstituted phenacenes have relatively large band gaps. We also notice from the band structures, that at $k = 0$, the energy levels of the two highest valence bands (HOCO and HOCO−1) are very close (Actually, these two bands correspond to the unfolded HOMO band at the LHS level). Similarly, the two lowest conduction bands (LUCO and LUCO+1) are almost equal (They correspond to the unfolded LUMO band at the LHS level). The orbital diagrams of the HOCO−1 and LUCO+1 are shown in Figure 5c,d, respectively. Note that the energy level of the HOCO is sensitive to the peripheral a-type bond length, while the HOCO−1 is more sensitive to the BLA of the *cis*-PA. Similarly, the LUCO is sensitive the BLA of the *cis*-PA, while the LUCO+1 is more sensitive to the peripheral a-type bond length. For substituted phenacenes, the HOCO might correspond to the orbitals shown in either part a or part c of Figure 5, depending on how the geometry is affected by substitution. Likewise, the LUCO might correspond to the orbitals shown in either part b or part d of Figure 5.

Phenacenes and helicenes have similar local connectivities.[53] The two series are closely related with respect to the corresponding bond distances as discussed in the previous section, as well as with respect to other properties, such as total energies and magnetic susceptibilities.[17] Intuitively, the band gap of phenacene is expected to be smaller than that of helicene considering the nonplanarity of the latter. However, the predicted band gap for helicene at B3LYP/6-31G* level is 0.7 eV smaller than that for phenacene despite the nonplanarity of helicene. Our interest in the band gap difference between the two systems lies in the fact that it might provide an opportunity to better understand the electronic structure of conjugated helicenes. The LHS method offers a good starting point to examine the topological effect on the band gap difference between the two systems. The unit cell and bond connectivities are shown in Figure 6. The LHS band structure should not be directly compared to the DFT calculations. However, the trend between the gap values predicted for the two systems using LHS is the opposite of that found in the DFT calculations as can be seen in Table 4. According to the closeness of the two LHS values, phenacene and helicene should have similar band

(53) Gimarc, B. M. *Gazz. Chim. Ital.* **1989**, *119*, 1.

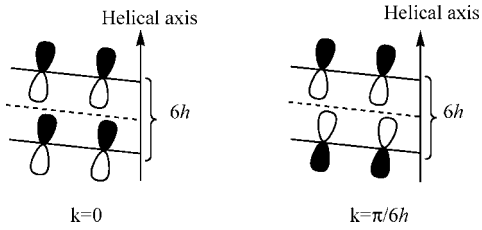

Figure 7. Schematic orbital overlap diagram across helical pitch at $k = 0$ and $\pi/6h$ ($a = 6h$, assuming a 6_1 symmetry).

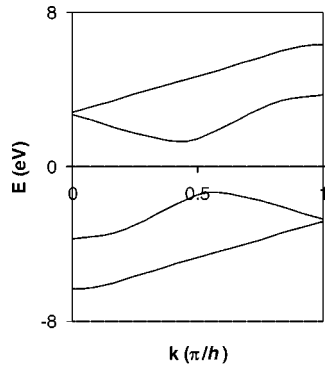

Figure 8. π-Band structure of helicene calculated with the LHS model. Two occupied and two empty bands are shown.

gaps. Therefore, there are some other factors affecting the band gap difference between the two systems.

We notice from Figure 3 that the HOMO−LUMO gaps of helicenes and phenacenes coincide for the systems with 3, 4 and 5 rings, and starting from 6 rings, the gaps started to diverge from each other. The differences become larger with the increasing number of rings. We can see from the structure of helicenes that the $\pi-\pi$ orbital overlap across the helical pitch starts from hexahelicene, which corresponds to one helical turn. With the assumption of 6_1 symmetry as discussed above, the crystal orbitals overlap out of phase across the helical pitch at $k = 0$ as shown in Figure 7, because the superposed π orbitals between neighboring unit cells are in phase due to translational symmetry, no matter how the orbitals look like in each translational unit cell (one full helical turn). Correspondingly, the crystal orbitals overlap in phase at $k = \pi/6h$ (or $k = \pi/a$, $a = 6h$), since the superposed π orbitals between neighboring unit cells are out of phase. DFT calculations indicate that the HOCO is located very near to $k = 0$, leading to an out of phase $\pi-\pi$ overlap, and accordingly, the energy level is raised due to the orbital interaction across the pitch. The LUCO is located very close to $k = \pi/6h$, leading to an in phase $\pi-\pi$ overlap, and therefore the energy level is lowered.

The LHS band structure is shown in Figure 8, which indicates that the HOCO and LUCO are both located around $k = \pi/2h$. Figure 9a shows the 6-fold back-folded band structure at the LHS level. Figure 9b shows the energy band structure from the PBC−DFT calculation with 6_1 symmetry. Note that the band crossings are a result of the backfolding because the levels that cross correspond to different k-value in the extended BZ as shown in Figure 8.

The two band structures are similar, which means that most of the band features are predicted rather well with the LHS model excluding the π orbital overlap effect across the pitch.

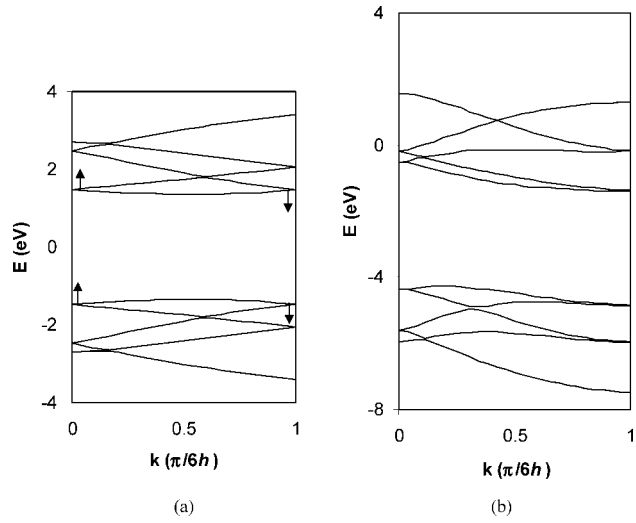

Figure 9. Part of the calculated band structures of helicene. (a) After back-folding of the LHS bands; (b) PBC with 6_1 symmetry at the B3LYP/6-31G* level. Five occupied and five empty bands are shown.

We separated the factors affecting the energy level of the PBC−DFT calculated bands into two parts. One arises from the conjugation along the helicene chain, which can be approximately evaluated at the LHS level according to the similarity between the back-folded LHS bands and DFT bands. The other part comes from the $\pi-\pi$ orbital overlap across the helical pitch, which is automatically included in the PBC calculation at the DFT level. We notice that at the LHS level, the valence and the conduction bands after back-folding are very flat meaning that the bands would be approximately independent of k for the valance and the conduction bands. However, the overlap across the helical pitch is highly dependent on k as discussed in connection with Figure 7. Compared to the LHS bands, the energy level of the conduction band moves up and is lowered at around $k = 0$ and $k = \pi/6h$, respectively, as indicated by the arrows in Figure 9a. Similarly, the energy level of the valance band moves up and is lowered at around $k = 0$ and $k = \pi/6h$, respectively. Therefore, the HOCO moves toward $k = 0$, and the LUCO moves toward $k = \pi/6h$ compared to the LHS bands, as shown in Figure 9b. Consequently, the band gap of helicene is significantly reduced by the π orbital overlap across the helical pitch.

Geometry of Thienoacenes and C_2S Helicenes. First, we compare the experimental and fully optimized geometries of [5]thienoacenes[26a] and C_2S [11]helicene,[28b] which are the largest oligomers available in CSD for these two systems. The bond distances in the middle rings are used for comparison, as illustrated in Figure 10. Table 5 lists selected bond distances from X-ray and the optimized geometry for the two molecules.

Accordingly, the corresponding CC bond distances fit very well between experiment and the optimized geometry. The optimized geometries for [7] and [11] C_2S helicene are in good agreement with those calculated at the similar level by Osuna et al.[54] In thiophenes, B3LYP/6-31G* systemati-

(54) Osuna, R. M.; Ortiz, R. P.; Hernandez, V.; Lopez Navarrette, J. T.; Miyasaka, M.; Rajca, S.; Rajca, A.; Glaser, R. *J. Phys. Chem. C* **2007**, *111*, 4854.

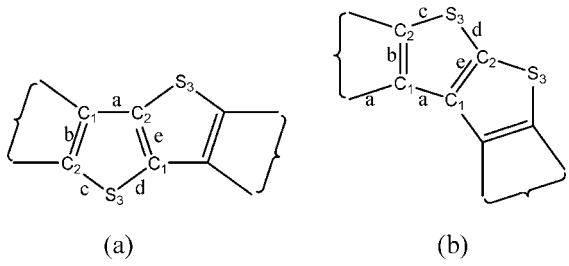

Figure 10. Illustration of bond distances in (a) infinite thienoacene; (b) infinite C_2S helicene. Numbering is given for two adjacent unit cells. Note the cisoid polyacetylene-like chain in (a).

Table 5. Central Bond Distances for [5]Thienoacene and C_2S [11]Helicene from Crystal Structure and B3LYP/6-31G* Geometry Optimization

		unit (Å)				
		a	b	c	d	e
[5]thienoacene	optimization, C_{2v}	1.419	1.395	1.756	1.756	1.395
	X-ray[26a]	1.426	1.399	1.735	1.735	1.399
C_2S [11]helicene	optimization, C_2	1.455	1.393	1.746	1.746	1.393
	X-ray[28b]	1.454	1.381	1.733	1.728	1.374

Table 6. Optimized Bond Distances for Infinite Thienoacene Using PBC and for [25]Thienoacene and C_2S [30]Helicene at the B3LYP/6-31G* Level[a]

	a (Å)	b (Å)	c (Å)
thienoacene (PBC−DFT)	1.416	1.397	1.756
[25]thienoacene	1.416	1.397	1.756
C_2S helicene(PBC−DFT)[b]	N/A	N/A	N/A
C_2S [30]helicene	1.457	1.394	1.742

[a] The bond distances correspond to the middle ring as labeled in Figure 10. [b] The PBC calculation is not practical for C_2S helicene because of the large number of atoms in the unit cell at the 26_3 screw axis of symmetry.

cally overestimates the CS bond lengths, e.g., for thiophene we obtained 1.736 Å as compared to MP2 calculations (1.718 Å) and the experiment (1.714 Å).[55] This is also the case for thienoacenes and C_2S helicenes. Based upon the good match, we assume that B3LYP/6-31G* is applicable to these types of systems. Table 6 lists the bond distances of thienoacene optimized with PBC at B3LYP/6-31G*. A longer oligomer, [25]thienoacene, was also optimized at the same level of theory in order to examine the PBC constraint on the geometry optimization. The bond distances in the middle ring of the oligomer were compared with the corresponding distances optimized using PBC. The two approaches give exactly the same bond distances for thienoacene as shown in Table 6. According to the optimized geometry of oligomers, C_2S helicene approaches an approximate 26_3 symmetry ($\theta = 6\pi/26$) as the number of rings increases. A translational vector can be defined with each unit cell containing 26 C_2S units. However, the large number of atoms per such a unit cell prohibits PBC calculations at the B3LYP/6-31G* level for this system. Such a 26_3 symmetry leads to interdigitated S···S contacts across the helix pitch, and thereby good overlap between sulfurs is not expected. The a-type CC bonds is the longer of the two for both types of systems, but the difference between the a-type and b-type bonds is very small in the thienoacene case.

(55) Cuff, L.; Kertesz, M. *J. Chem. Phys.* **1997**, *106*, 5541.

Table 7. Calculated and Experimental Band Gaps for Infinite Thienoacene and C_2S Helicene

	unit (eV)					
				experiment		
	LHS	extrapolation[a]	PBC−DFT[b]	*c*	*d*	*e*
thienoacene	2.25	2.15	2.25	2.25	2.21	2.33
C_2S helicene	4.12	4.1	N/A	N/A	N/A	N/A

[a] HOMO−LUMO gap extrapolation calculated at the B3LYP/6-31G* level. Extrapolation range: [3]−[40]thienoacene; C_2S [3]−[30]helicene. [b] PBC calculation at B3LYP/6-31G* level. [c] The band gap was extrapolated with HOMO−LUMO gaps versus the reciprocal of the number of rings. The HOMO−LUMO gap points were obtained from the UV−vis spectra of [3]-, [5]-, [7]thienoacenes.[26a] [d] The band gap was extrapolated with HOMO−LUMO gaps versus the reciprocal of the number of rings. The HOMO−LUMO gap points were obtained from the UV−vis spectra of [4]-, [6]-, [8]thienoacenes.[26b] [e] Experimental HOMO−LUMO gaps from ref 26b were linearly fitted as a function of the reciprocal number of π electrons.

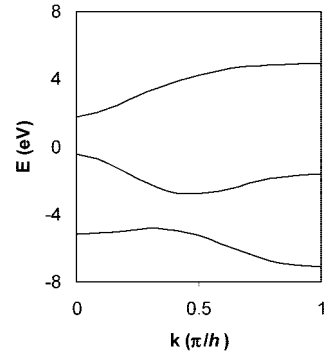

Figure 11. Unfolded π-band structure of thienoacene calculated by LHS. Two occupied bands and one empty band is shown.

Band Gap Analysis for Thienoacenes and C_2S Helicenes. The band gaps obtained from extrapolation and PBC calculations are listed in Table 7 for thienoacenes and thiohelicenes. Thienoacene has a much larger band gap than C_2S helicene for the same number of rings. Topology is an important factor to be considered in band gap engineering of organic conductors or semiconductors.[56] There are topological reasons for such a large band gap difference between these two systems based on a qualitative orbital analysis. At first sight, it seems that the local bond connectivity is very similar, and the optimized and experimental geometry show similar bond delocalization for the two systems as shown in Table 5 and Table 6. However, a *cis*-PA-like backbone can be defined for polythienoacene, but not for C_2S helicene chain. The backbone of *cis*-PA can be considered as the starting point of the analysis of the electronic structures for polythiophene[57] and polythienoacene,[25] but not for C_2S helicene.

Similar to the band gap discussion on hydrocarbon system, the semiempirical LHS model was used to clarify how the bond connectivity affects the band gaps of thienoacene and C_2S helicene. The LHS calculated band structure of thienoacene is shown in Figure 11, which indicates a direct band gap at $k = 0$. The back-folded LHS band structure and the DFT band structure are shown in Figure 12a,b, respectively. Both of them indicate a similar direct band gap at $k = 0$ in the reduced BZ.

(56) Seo, D.-K.; Hoffmann, R. *Theor. Chem. Acc.* **1999**, *102*, 23.
(57) Kertesz, M.; Lee, Y. S. *J. Phys. Chem.* **1987**, *91*, 2690.

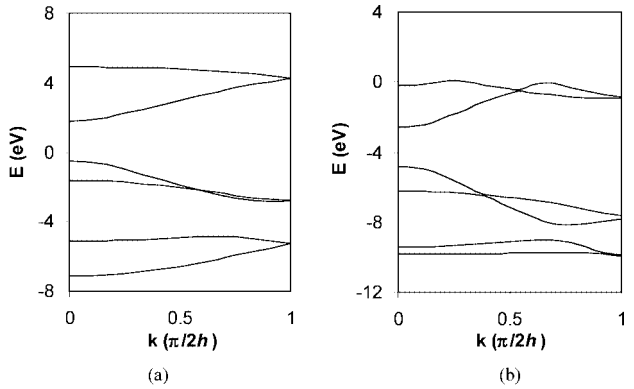

Figure 12. Band structures of thienoacene. (a) Back-folded bands at the LHS level; (b) PBC at B3LYP/6-31G* level. Four occupied and two empty bands are shown.

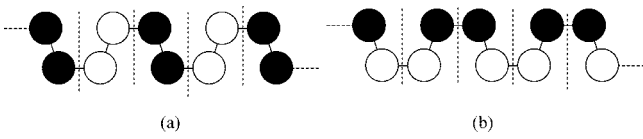

Figure 13. Orbital diagrams corresponding to the *cis*-PA bands at $k = 0$ in thienoacene. (a) HOCO; (b) LUCO.

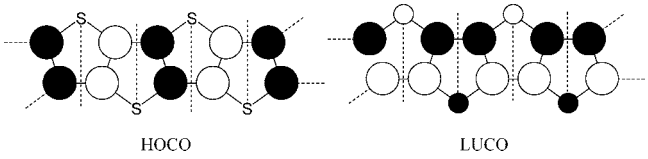

Figure 14. Orbital diagrams of HOCO and LUCO of thienoacene at $k = 0$.

The following orbital analysis was based on the unfolded band structure (in the extended BZ) calculated by LHS. The backbone of thienoacene is divided into two parts: one is a set of sulfur atoms, and the leftover is reminiscent of *cis*-PA. Consequently, the energy bands can be approximately classified as PA bands and sulfur bands, which strongly mix with each other at certain k points. Figure 13a,b illustrates the orbital diagrams corresponding to the HOCO and the LUCO of *cis*-PA at $k = 0$.

Note that the sulfur π-orbitals do not mix with the PA-like HOCO at $k = 0$. However, the sulfur π-orbitals mix with the PA LUCO at $k = 0$ with antibonding character between the π-orbitals of sulfur and the carbons directly connected to it raising the LUCO energy level. Figure 14 shows the orbital diagram of the HOCO and the LUCO of thienoacene. Thus, similar to ploythiophene,[57] the band gap of thienoacene has two components, i.e. the S−C antibonding interaction in LUCO and the BLA of *cis*-PA backbone. The former factor enlarges the band gap. According to optimized bond lengths as shown in Table 6, the BLA along the PA is small for thienoacene. Therefore, the band gap is not very large with the value of 2.2 eV.

Figure 15 shows the LHS band structure corresponding to the carbon backbone. It indicates an indirect band gap with the HOCO at $k = \pi/h$ and LUCO at $k = 0$. The respective orbitals are shown in Figure 16. The small coefficients on the inner carbons lead to a band gap larger than that of thienoacene due to the lack of efficient conjugation pathway in C_2S helicene.

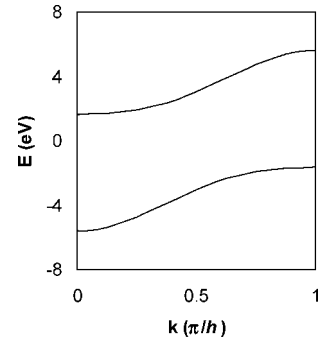

Figure 15. LHS calculated band structure of the carbon backbone of C_2S helicene.

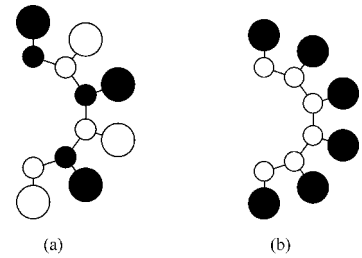

Figure 16. Schematic orbital diagrams corresponding to the carbon backbone in C_2S helicene. (a) HOCO at $k = \pi/h$; (b) LUCO at $k = 0$.

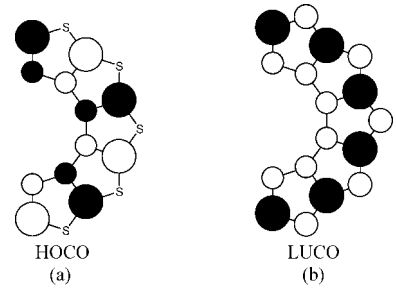

Figure 17. Orbital diagram of C_2S helicene with sulfur contribution. (a) HOCO at $k = \pi/h$; (b) LUCO at $k = 0$.

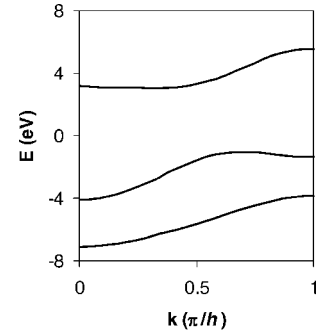

Figure 18. LHS calculated π-band structure of C_2S helicene. Two of the bands are occupied.

The HOCO and LUCO, after coupling with the sulfur π-orbitals, are shown in Figure 17. Similar to thienoacene, there is no contribution from sulfur to the HOCO due to the additional mirror planes of symmetry, but the sulfur π-orbitals couple with the LUCO. This finding is supported by the band structure of C_2S helicene as shown in Figure 18, where the energy level of LUCO is raised compared to the LUCO of carbon backbone (Figure 15) due to the S−C antibonding interaction.

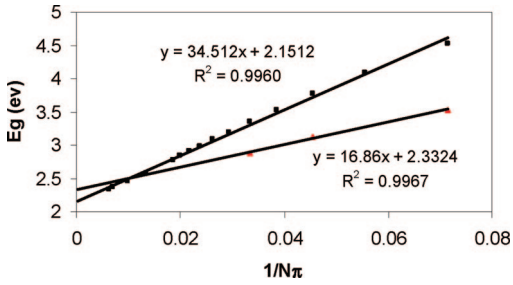

Figure 19. B3LYP/6-31G* calculated and experimental HOMO−LUMO gaps for thienoacene as a function of $1/N_\pi$. Linear fits were used for both calculated and experimental values, and corresponding statistics are shown. The experimental HOMO−LUMO gaps was measured with the UV−vis spectra of [4]-, [6]-, and [8]thienoacenes.[26b] (Diamonds: calculated HOMO−LUMO gaps; squares: experimental values.)

Apart from the HOCO−LUCO mixing for C_2S helicene, which enlarges the band gap compared to thienoacene, we also notice from the optimized geometry, that the a-type bonds are much shorter for thienoacene (1.416 Å) than that for C_2S helicene (1.457 Å). This leads to an even higher HOCO level for thienoacene due to antibonding character on these bonds. Similarly, the shorter a-type bonds distance makes the LUCO level even lower for thienoacene than that for C_2S helicene. Consequently, the band gap of thienoacene is further reduced compared to that of C_2S helicene.

Due to the helical structure of C_2S helicene, the π orbital overlap across the helical pitch might affect the band gap, which the above analysis did not yet include. As we discussed above, there is no contribution from sulfur to the HOCO. Furthermore, the in phase and out of phase $\pi-\pi$ overlap between the superposing rings nearly cancel. Therefore, the energy level of the HOCO is not affected by the π-orbital overlap across the helical pitch. For the LUCO, there is significant contribution from sulfur. Although the distance between the mean planes of superposing rings is approximately 3.70 Å, a value close to the van der Waals distance of sulfur, an efficient overlap is not possible because of the overall approximate 26_3 structure, which creates an interdigitated network of sulfur atoms with S···S contacts calculated at 4.15−4.20 Å. Therefore, the sulfur π-overlap is not significant for the energy level of the LUCO. The out of phase $\pi-\pi$ overlap from the superposing carbon atoms might raise energy level of LUCO. However, the overlap is not efficient due to the $\pi-\pi$ overlap cancelation between the imperfectly superposing rings. The calculated S···S distances (4.15−4.20) is smaller than the X-ray values at 4.43−4.71 for [11]C_2S helicene, but still larger than the van de Waals distance of sulfur. Since both experiment and DFT contacts are too large for effective overlap, the dispersion effect is negligible on the band structure. Accordingly, we suggest that the band gap is not significantly influenced by the orbital overlap across the helical pitch. We also learn from the orbital diagram of C_2S helicene, that nonpalanarity further enlarges the band gap.

The calculated HOMO−LUMO gap extrapolation for thienoacene is shown in Figure 19.

The points were linearly fitted up to [40]thienoacene with an excellent correlation coefficient. The extrapolated band gap is 2.15 eV, which is close to 2.25 eV from the PBC calculation. If longer oligomers were included, the band gap from the two methods should coincide. The experimental HOMO−LUMO gaps are also shown in Figure 19 for [4]-, [6]-, and [8]thienoacenes.[26b] We notice that these values are systematically lower than the calculated values. The possible reason is that our calculation of the HOMO−LUMO gaps ignores important correlation effects. However, the difference between calculated and experimental values decreased with the increase of the number of rings. The experimental HOMO−LUMO extrapolation gave band gap of 1.99 eV, which is very similar to that from the calculation.

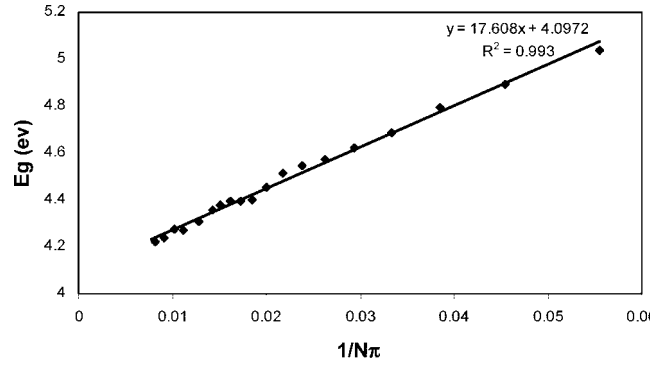

Figure 20. B3LYP/6-31G* calculated HOMO−LUMO gaps for C_2S helicene as a function of $1/N\pi$. A linear fit and corresponding statistics are also shown.

Table 8. Selected Bond Distances for Hexathia[11]heterohelicene from Crystal Structure and Geometry Optimization at the B3LYP/6-31G* Level[a]

	unit (Å)							
	a	b	c	d	e	f	g	h
X-ray[59]	1.393	1.390	1.379	1.392	1.420	1.416	1.449	1.741
optimization	1.418	1.400	1.389	1.400	1.418	1.429	1.459	1.759

[a] The bonds are labeled according to Figure 21a.

The HOMO−LUMO extrapolation for C_2S helicene is shown in Figure 20, in which oligomers up to 30 rings were used. The extrapolated band gap is 4.10 eV, which is much larger than that of thienoacene just as predicted by the qualitative orbital analysis. The optical absorption maxima for C_2S [7]helicene is around 4.85 eV,[28a] which fits well with our calculation. When the absorption onset was used, the optical gap is 3.55 eV for C_2S [11]helicene, which is smaller than our calculation, 4.51 eV. However, the optical gap corresponding to the absorption maxima fit much better with our calculation. The justification for the difference between the calculated and experimental value is similar to that for helicene. The possible reason is due to the nearly degeneracy of the HOMO level, which reduces the band gap due to vibronic coupling.[54] The other possible reason is that λ_{onset}, instead of λ_{max} was used in the experiment. The problems using λ_{onset} is that this value might corresponds to adiabatic transition energy which is lower than vertical excitation at λ_{max}. The HOMO−LUMO gap approximation corresponds to the λ_{max}, and hence it is smaller than experimental values using λ_{onset}.

Geometry Optimization and Band Gap for Thiaheterohelicenes. The geometries from optimization and X-ray are listed in Table 8 for hexathia[11]heterohelicene. The similar calculation has been done for tetrathia[7]heteroheli-

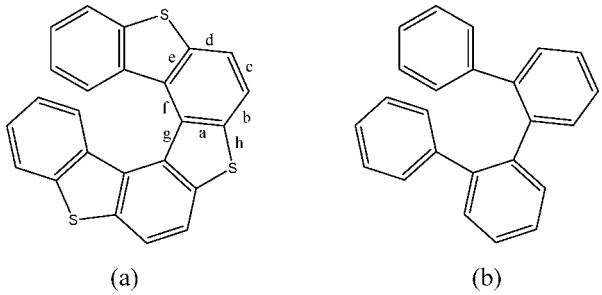

Figure 21. (a) Bond labeling for thiaheterohelicene. (b) Schematic structure of helical poly(*o*-phenylene).

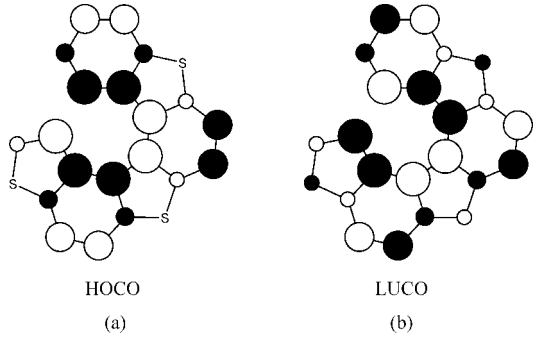

Figure 22. Illustration of the HOCO and LUCO at $k = \pi/h$ for thiaheterohelicene.

cenehelicene at B3LYP/6-31G**[58] and gave same bond distances as our calculation at B3LYP/6-31G*. The CC bonds opposite to sulfur atoms are the longest and peripheral bonds are the shortest just as is the case of the helicenes and C_2S helicene. In thiaheterohelicene, a thiophene ring is right above a benzene ring, and it tends to adopt an approximately 7_2 symmetry with the increasing number of rings. For hexathia[11]heterohelicene, the distance between the centroids of the overlapping benzene and thiophene rings is 3.681 Å and 3.893 Å according to the optimized and X-ray geometry, respectively. Such distance for the optimized octathia[15]heterohelicene is 3.803 Å.

Thiaheterohelicene is analogous to helical poly(*o*-phenylene) with the removal of sulfur (Figure 21b). Helical poly(*o*-phenylene) can be used as a starting point for a qualitative orbital analysis. The HOCO and LUCO are shown in Figure 22. The sulfur π-orbitals are decoupled from the HOCO of poly(*o*-phenylene) due to symmetry, but their antibonding interactions with neighboring carbons raise the LUCO band and the band gap is enlarged similarly to C_2S helicene. We also notice that the bonds opposite to the sulfur atoms have antibonding character in the HOCO, and bonding character in the LUCO. Compared with poly(*o*-phenylene), the sulfur atoms tend to reduce the CC bonds opposite to the sulfurs, and thereby reduce the bond length alternation of the PA-like chains composed of the inner carbon atoms. Therefore, the band gap is reduced.

Figure 23 shows the HOMO−LUMO gap extrapolation for thiaheterohelicene. The extrapolated band gap is 2.52 eV, which is the smallest among the helical systems covered in this study, although according to its composition, thiaheterohelicene is between the two large band gap systems, helicene and C_2S helicene. The electrochemical energy gaps have been measured with the values of 3.46 and 3.14 eV,[60] respectively, for tetrathiathetero[7]helicene and hexathiahetero[10]helicene, which fit fairly well with our calculations.

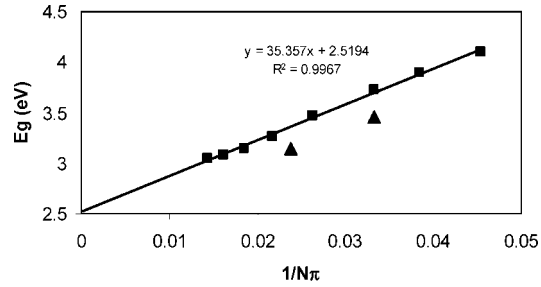

Figure 23. B3LYP/6-31G* calculated HOMO−LUMO gaps (squares) for thiaheterohelicenes as a function of $1/N\pi$. Electrochemical gaps[60] for tetrathiahetero[7]helicene and hexathiahetero[10]helicene are also shown (triangles).

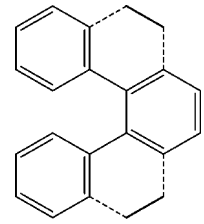

Figure 24. Illustration of the separation of helicene into poly(*o*-phenylene) and ethylene. The bold bonds are the ethylene fragments.

The smaller band gap of thiaheterohelicenes compared to C_2S helicene can be easily rationalized due to the lack of effective conjugation pathway of the latter. For the comparison between thiaheterohelicene and helicene, the orbital analysis of helicene also starts from poly(*o*-phenylene), as shown in Figure 24, where helicene is divided into two parts. Correspondingly, the energy bands can be classified as poly (*o*-phenylene) bands and ethylene bands. Note, that the HOCO of poly (*o*-phenylene) couples with the LUMO of ethylene at $k = \pi/h$, thereby the HOCO is stabilized. However, for thiaheterohelicene, such stabilization is not possible. Meanwhile, for helicene, the LUCO of poly (*o*-phenylene) mixes with the HOMO of ethylene, therefore, the LUCO is raised. This is similar to the destabilization effect of the sulfur band on the LUCO of thiaheterohelicene. Overall, the band gap of thiaheterohelicene is reduced compared to helicene. According to the orbital diagram of HOCO and LUCO, the in phase and out phase π-orbital overlaps cancel with each other across the superposed benzene and thiophene rings.

Conclusions

Phenacene and isomeric helicene have similar bond connectivities, and DFT calculations indicated that corresponding bond distances are nearly identical for the polymers of the two systems. According to geometry optimization for

(58) Daul, C. A.; Ciofini, I.; Weber, V. *Int. J. Quantum Chem.* **2003**, *91*, 297.
(59) Nakagawa, H.; Yoshino, J.; Yamada, K.; Shiro, M. *Chem. Lett.* **2003**, *32*, 90.
(60) Bossi, A.; Falciolab, L.; Graiffc, C.; Licandroa, E.; Maioranaa, S.; Mussinib, P. R.; Rigamontid, C.; Tiripicchio, A. To be published.

a series of oligomers of helicene, the infinite helicene tends to adopt a close to 6_1 symmetry. Despite of the nonplanarity, both PBC calculation and HOMO−LUMO gap extrapolation at B3LYP/6-31G* level showed that the band gap of helicene is ∼0.7 eV smaller than that of phenacene. With the combination of band structure and orbital analysis, we concluded that the $\pi-\pi$ overlap across the helical pitch reduces the band gap for helicene compared to planar phenacenes.

The band gap of C_2S helicene, 4.10 eV, is much larger than that of the isomeric thienoacene, 2.15 eV. Qualitative orbital analysis showed that the larger band gap difference is due to the lack of an effective conjugation path for C_2S helicene. In addition, the optimized geometry indicated a longer CC bond opposite to sulfur for C_2S helicene than that for thienoacene, which further enlarged the band gap difference between the two systems. Due to the approximately 26_3 helical structure found here as the most likely structure for C_2S helicene, the sulfur atoms across the pitch form an interdigitated network. The result of this structure leads to a reduced $\pi-\pi$ overlap across the helical pitch.

The extrapolated band gap of 2.52 eV for thiaheterohelicene is the smallest among the helical systems covered in this study. The sulfur affects the band gap in two ways. Orbital analysis reveals that sulfur raises the energy level of LUCO and enlarges the band gap. On the other hand, it reduces the bond length alternation of the PA-like chains composed of the inner carbons, thereby further reducing the band gap. We find no evidence for a π-orbital overlaps significantly affecting the gaps of thiaheterohelicene.

We pointed out difficulties in performing periodic calculations on helical systems with large translational periods but also showed how to overcome these difficulties by using extrapolations from oligomer calculations.

Acknowledgment. Financial support from the National Science Foundation (Grant DMR-0331710) is gratefully acknowledged.

Supporting Information Available: Cartesian coordinates of the longest oligomers for each system covered in the paper; the HOMO−LUMO gaps; total energy of all the oligomers; Figure 1S for qualitative orbital analysis for infinite phenacene; Figure 2S for units cells used for PBC calculations; and Figure 3S of the band plot of phenacene in the extended BZ. This material is available free of charge via the Internet at http://pubs.acs.org.

CM702813S